ChemComm

Accepted Manuscript

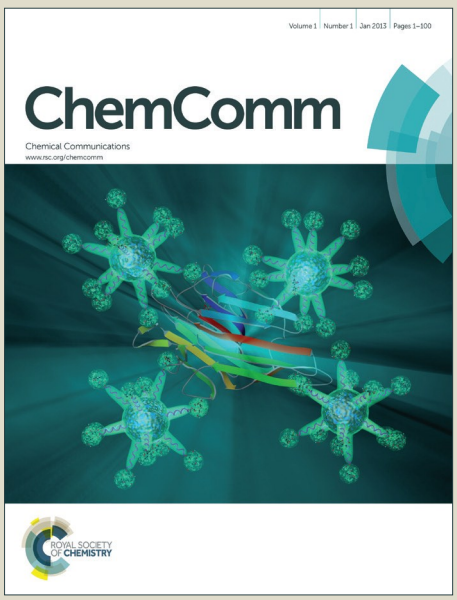

ROYAL SOCIETY OF CHEMISTRY

www.rsc.org/chemcomm

ChemComm

RSCPublishing

COMMUNICATION

Scalable synthesis of cubic $Cu_{1.4}S$ nanoparticles with long-term stability by laser ablation of salt powder

Cite this: DOI: 10.1039/xoxxoooooox

Y. Zhou, H. Liu, J. Yang, J. Mao, C. K. Dong, T. Ling and X. W. Du*

Received ooth January 2015,
Accepted ooth January 2015

DOI: 10.1039/xoxxoooooox

www.rsc.org/

Cubic $Cu_{1.4}S$ nanoparticles were synthesized on a large scale by laser ablation of salt powder dispersed in organic solvent. Metastable $Cu_{1.4}S$ phase formed under high temperature in reductive solvent and retained to room temperature due to the quenching effect of the pulsed laser. The cubic $Cu_{1.4}S$ nanoparticles show good stability after being exposed to ambient atmosphere for as long as 1 month.

Copper sulfides (Cu_xS, $1 \le x \le 2$), including several compounds with varied stoichiometries, e.g. Cu_2S (chalcocite), $Cu_{1.97}S$ (djurleite), $Cu_{1.8}S$ (digenite), $Cu_{1.4}S$ (anilite) and CuS (covellite), are promising for the application in thin film solar cells owing to their ideal band gaps, high absorption coefficient, nontoxicity, and elemental abundance.[1] Indeed, solar cells based on Cu_xS reached an efficiency as high as 10% in the early 1980s, however, the devices degraded remarkably in performance over a period of a few weeks due to the instability of the Cu_xS materials,[2] which has long been a bottleneck for the practical application of Cu_xS materials.[3] The theoretical calculation indicates that the instability arises from their high heat of formation. Particularly, the cubic structure possesses the highest heat of formation among all of Cu_xS phases.[4] Therefore, it remains a big challenge to produce stable cubic Cu_xS materials.[5]

The technique of laser ablation in liquid (LAL), which employs intensive pulsed laser to irradiate solid target immersed in liquid, is well known for its facile and green synthesis of nanostructures.[6] More intriguingly, LAL can generate extremely high temperature and pressure, following with a quenching process which may stabilize the high-temperature phases.[7] Common LAL technique adopts metal or compound as targets. Because of the high boiling points of metal or compound targets, a majority of laser energy is consumed on heating target, thus the yield rate of LAL is very limited.[15] In comparison, ionic salt targets own lower boiling points due to the weak ionic bonds, which extremely facilitates the scalable synthesis. However, only few works deal with salt targets (e.g. $NiCl_2$, perovskites and organic-metal salts). [1a, 8].

Herein, we employed a salt target, copper acetylacetonate ($Cu(acac)_2$) powder, and dimethyl trisulfide (DMTS) for LAL synthesis of Cu_xS materials. We found that the LAL can create a reductive environment making for $Cu_{1.4}S$ nanoparticles. Especially, the fierce synthetic conditions (high temperature, high pressure and high cooling rate) result in an unusual cubic phase with long-term stability, which is very crucial for solar cell application. Moreover, our process displays several advantages, namely, the utilization of salt target helps raise production; the superfast reaction rate and the quenching effect depress the possible oxidation by ambient gas, in favour of the production of pure $Cu_{1.4}S$ nanoparticles; the synthesis proceeds under ambient conditions, thus being simpler and greener than conventional synthetic routes.[1a]

As shown in Figure 1a, the product from salt target displays a deep black colour, while that obtained by using metal target and the same laser parameters exhibits a light brown colour, implying that the salt target is advantageous on the scalable synthesis. Such a speculation is confirmed by SEM image shown in Figure 1b, where massive aggregates of nanoparticle are found in the product of salt target. TEM image presents uniform nanoparticles with a size distribution of 8.4±1.1 nm (Figure 1c and Figure S1 in supporting information). The dispersion of nanoparticles depends on the dosage of oleic acid (OA), and well dispersed nanoparticles can be achieved at a proper amount of OA (see Figure S2 in supporting information). The selected area electron diffraction (SAED) pattern inserted in Figure 1c accords with a face-centred cubic phase, being consistent with the XRD result shown in Figure 1d. Compared with standard cubic digenite ($Cu_{1.8}S$, JCPDS 24-0061), the diffraction peaks shift slightly toward high angle direction by 0.8°, indicating a relative decrease of the lattice parameters. High resolution TEM (HRTEM) image in the lower inset of Figure 1c presents lattice fringes with a spacing of 0.275 nm, corresponding to (111) planes of cubic structure. The composition information are obtained by XPS and EDS analysis (Figures 1e and 1f).The intensive peaks in XPS profile at 931.9 and 951.9 eV are assigned to Cu $2p_{3/2}$ and Cu 2p1/2 of Cu^{2+}, ions [9] while those at 933 and 953 eV correspond to Cu 2p3/2 and Cu 2p1/2 of Cu^+ ions, respectively.[10] The Cu^+/Cu^{2+} ratio are calculated to be 1.5, hence the formula of Cu_xS is written as $0.75Cu_2S \bullet CuS$. After normalizes the number of S atoms to 1, the final value X is calculated to be 1.42, which is accurately close to theoretical value 1.4, indicating a composition of $Cu_{1.4}S$ (anilite). Moreover, the quantitive EDS analysis gives a Cu/S ratio of 1.35, which is close to the stoichiometric ratio of $Cu_{1.4}S$.

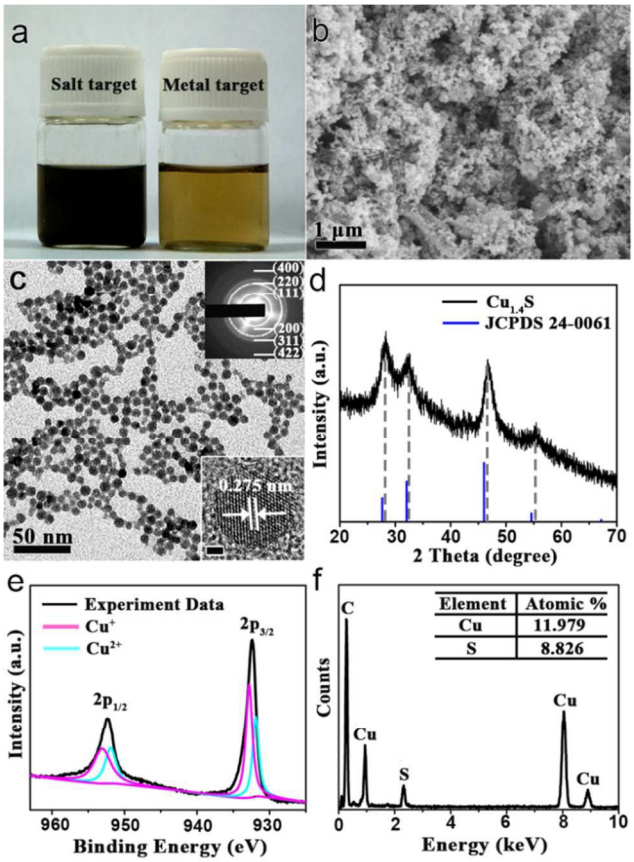

Figure 1. Characterization on the products. (a) Optical images of the products from salt and metal targets, respectively, via laser ablation. (b) SEM, (c) TEM image, (d) XRD pattern, (e) XPS spectrum, and (f) EDS profile of the product by laser ablation of Cu $(acac)_2$ powder, top and bottom insets in (c) are corresponding SAED pattern and HRTEM image (scale bar represents 2 nm).

To identify the uniqueness of LAL on the synthesis of metastable cubic anilite, we performed the solvothermal synthesis by adopting the same precursors for laser ablation. The solution of $Cu(acac)_2$ and DMTS was heated to 473 K and the temperature was held for 1 hour. The product shows several features distinct from $Cu_{1.4}S$ nanoparticles via LAL. First, the product presents an urchin-like morphology at submicron scale (Figure S3a) with single-crystal branches (Figure S3b). Second, the SEAD pattern (Figure S3c) and XRD profile (Figure S3d) are accurately indexed as hexagonal structure (JCPDS06-0464). Third, quantitive EDS analysis tells that the Cu: S ratio is closely 1:1, confirming the formation of CuS. These results indicate that wet-chemistry route gives rise to CuS urchins instead of $Cu_{1.4}S$ nanoparticles.

Since LAL process generates more reductive Cu^+ ions in $Cu_{1.4}S$ which is absent in the product (CuS) by solvothermal synthesis, we then supposed that LAL creates a unique reductive environment. To testify this hypothesis, CuS nanoparticles were dispersed into organic solvents (ethanol and acetone) and irradiated by the laser. XRD patterns clearly illustrate a phase transformation from hexagonal to cubic structure under laser irradiation in different organic solvents (Figure 2). On the other hand, the wet lead acetate testing paper became black when it was put on the opening of the

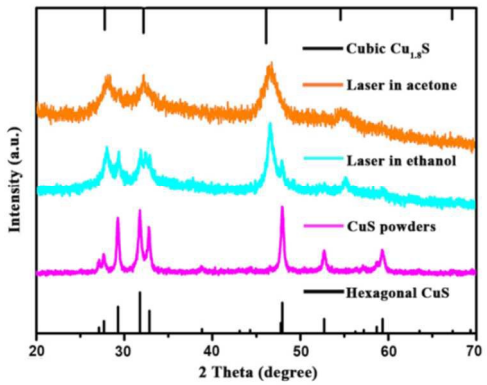

Figure 2. XRD patterns of the products by laser ablation CuS in ethanol and ecetone.

cuvette, suggesting the production of H_2S gas (see Figure S4 in supporting information). In contrast, CuS phase kept intact after being heated in ethanol at 473K for 1 hour (see Figure S5 in supporting information). The above results suggest that LAL possesses special capability on the reduction and dissociation of CuS.

On the basis of the above, we propose a possible mechanism for the formation of $Cu_{1.4}S$ nanoparticles in LAL process (Figure 3). First, $Cu(acac)_2$ powder can absorb the laser light efficiently (see Figure S5 in supporting information), be heated to a high temperature, and broken into Cu^{2+} and $acac^-$ ions (Figure 3a). Meanwhile, the surrounding solution is heated up rapidly, which causes the vaporization of organic solvent and the decomposition of DMTS into fragments including S^{2-} ions. In the high-temperature bubble, Cu^{2+} ions are partially reduced to Cu^+ ions by the solvent (e.g. ethanol) molecules. [11] Meanwhile, Cu^{2+}, Cu^+ and S^{2-} ions react rapidly to generate $Cu_{1.4}S$ nanoparticles with the lowest heat of formation among various cubic Cu_xS materials (Figure 3c).[4] Afterwards, the surrounding liquid medium quenches the hot cubic $Cu_{1.4}S$ nanoparticles to room temperature, and depresses phase separation into Dg and S (or Cv) phases (Figure 3d). Moreover, because the salt target is very easy to be dissociated, it can supply massive Cu^{2+} ions which motivate a violent reaction and produce a large amount of $Cu_{1.4}S$ nanoparticles.

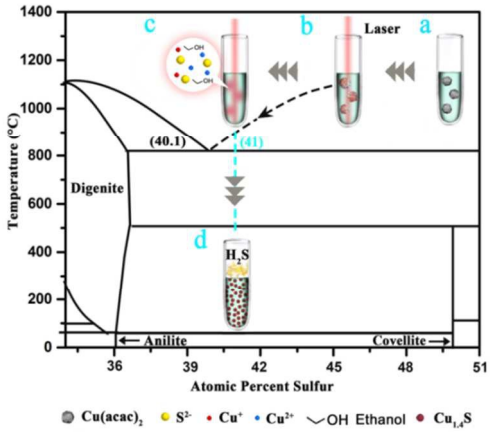

Figure 3. Phase diagram of Cu-S system.

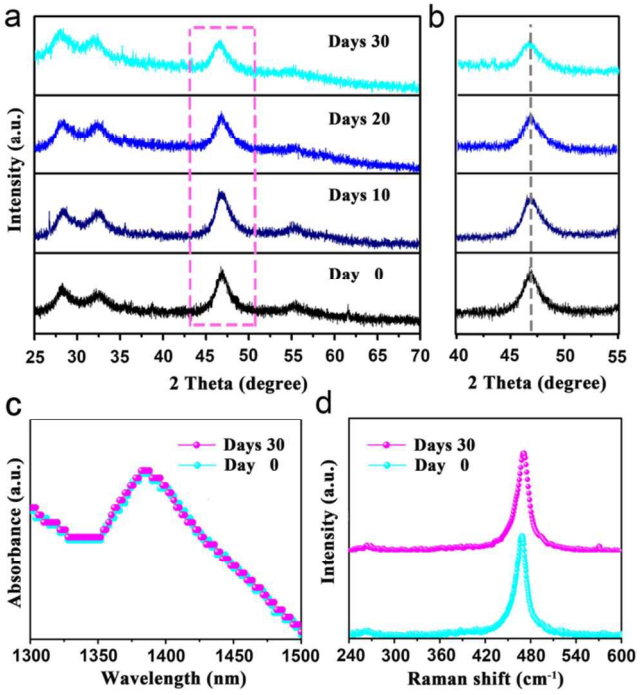

Figure 4. Characterization on the long-term stability of $Cu_{1.4}S$ nanoparticles. (a) XRD patterns of the sample stored in atmosphere for a month. (b) Enlarged area of (220) diffraction peak. (c) UV-Vis absorption spectra. (d) Raman spectra.

The above laser synthesis is not limited to the reaction between $Cu(acac)_2$ and DMTS, and can be extended to other systems. We employed copper acetate ($Cu(ac)_2$) and thioacetamide (TAA) as cooper and sulfur sources, respectively. Similarly, $Cu(ac)_2$ powder exhibit high absorption capability at 532 nm (Figure S5 in supporting information), thus $Cu_{1.4}S$ nanoparticles were obtained as well after the solution was irradiated by 532 nm laser (Figure S7). On the other hand, the solvothermal synthesis by using $Cu(ac)_2$ and TAA as precursors gave rise to hexagonal CuS nanoparticles (see Figure S7). These results are same with that of $Cu(acac)_2$-DMTS system, signifying that the laser synthesis can generate metastable phase which is hardly obtained by common solvothermal synthesis.

Finally, we tracked the long-term stability of cubic $Cu_{1.4}S$ nanoparticles by using XRD, absorption and Raman analyses. As shown in Figure 4a, no obvious change was found in XRD patterns after the sample was stored in ambient circumstance for a month (Figures 4a and 4b). In absorption spectra, Cu_xS materials possess a localized surface plasmon resonance (LSPR) at near infrared spectrum,[12] and the square of peak intensity is proportional to the hole concentration and composition change.[13] The LSPR peak of $Cu_{1.4}S$ nanoparticles around 1370 nm and its intensity keeps stable after one-month exposure to air (Figure 4c). The band shift in Raman spectrum can reflect the structural or compositional change of Cu_xS. As shown in Figure 4d, the Raman spectra show an intensive peak at 467.4 cm^{-1}, followed with a weak one at 260.8 cm^{-1}, according with the wavenumbers of Cu_xS ($1.12<x<1.8$) reported by R. Nagarajan et al.[14] Raman peaks keeps intact during the storage as well (Figure 4d). All of the above results jointly demonstrate the high stability of $Cu_{1.4}S$ nanoparticles.

Conclusions

Cubic $Cu_{1.4}S$ nanoparticles were synthesized by laser ablation of salt powder suspended in solution. The salt target can be broken into ions more easily than metal target, thus give rise to abundant ions for massive production of $Cu_{1.4}S$ nanoparticles. On the other hand, laser irradiation can result in active H atoms which favour the formation of $Cu_{1.4}S$ rather than CuS. Meanwhile, the as-prepared $Cu_{1.4}S$ nanoparticles possess a long-term stability, which is essential for solar cells applications. Hence, laser irradiation of salt target was demonstrated as a powerful strategy for massive production of novel materials.

This work was supported by the National Basic Research Program of China (2014CB931703), and the Natural Science Foundation of China (Nos. 51471115 and 51171127).

Notes and references

Institute of New-Energy Materials, School of Materials Science and Engineering, Tianjin University, Tianjin 300072, People's Republic of China
* Address correspondence to maojing@tju.edu.cn; xwdu@tju.edu.cn
Electronic Supplementary Information (ESI) available: [experimental details, statistics of $Cu_{1.4}S$ nanoparticles, Tem images about OA concentration on formation of $Cu_{1.4}S$ products, characterizations on the heating nanostructures of CuS nanobranches, picture of lead acetate testing paper after laser ablation mixture; UV-Vis absorption of $Cu(acac)_2$ and $Cu(ac)_2$ raw powders , characterization of laser and heating products obtained in $Cu(ac)_2$ and TAA system]. See DOI: 10.1039/c000000x/ 2007, 76

1. (a) C. Pan, S. Niu, Y. Ding, L. Dong, R. Yu, Y. Liu, G. Zhu and Z. L. Wang, *Nano Lett*, 2012, **12**, 3302; (b) Y. Wu, C. Wadia, W. L. Ma, B. Sadtler, a. A. P. Alivisatos, *Nano Lett*, 2008, **8**(8): 2551-2555.
2. (a) L. D. Partain, P. S. McLeod, J. A. Duisman, T. M. Peterson, D. E. Sawyer and C. S. Dean, *J. Appl. Phys*, 1983, **54**, 6708; (b) F. Pfisterer, *Thin Solid Films*, 2003, **431-432**, 470.
3. (a) A. B. F. Martinson, J. W. Elam and M. J. Pellin, *Appl Phys Lett*, 2009, **94**, 12; (b) P. Lukashev, W. R. L. Lambrecht, T. Kotani and M. van Schilfgaarde, *Phys. Rev. B*, 2007, **76**(19) : 195202.
4. Q. Xu, B. Huang, Y. Zhao, Y. Yan, R. Noufi and S.-H. Wei, *Appl Phys Lett*, 2012, **100**, 061906.
5. (a) D. J. Chakrabarti and D. E. Laughlin, *Bulletin of Alloy Phase Diagrams*, 1983, **4**, 254; (b) A. B. F. Martinson, S. C. Riha, E. Thimsen, J. W. Elam and M. J. Pellin, *Energ. Environ. Sci*, 2013, **6**, 1868; (c) L. Liu, H. Zhong, Z. Bai, T. Zhang, W. Fu, L. Shi, H. Xie, L. Deng and B. Zou, *Chem. Mat.*, 2013, **25**, 4828; (d) T. Machani, D. P. Rossi, B. J. Golden, E. C. Jones, M. Lotfipour and K. E. Plass, *Chem. Mat.*, 2011, **23**, 5491; (e) M. Lotfipour, T. Machani, D. P. Rossi and K. E. Plass, *Chem. Mat.*, 2011, **23**, 3032.
6. H. Zeng, X.-W. Du, S. C. Singh, S. A. Kulinich, S. Yang, J. He and W. Cai, *Adv. Funct. Mater.*, 2012, **22**, 1333.
7. (a) K. Y. Niu, J. Yang, S. A. Kulinich, J. Sun, H. Li and X. W. Du, *J. Am. Chem. Soc.*, 2010, **132**, 9814; (b) K. Y. Niu, H. M. Zheng, Z. Q. Li, J. Yang, J. Sun and X. W. Du, *Angewandte Chemie*, 2011, **50**, 4099-4102; cJ. Yang, T. Ling, W. T. Wu, H. Liu, M. R. Gao, C. Ling, L. Li and X. W. Du, *Nat Commun*, 2013, **4**, 1695; (d) H. Liu, P. Jin, Y. M. Xue, C. Dong, X. Li, C. C. Tang and X. W. Du, *Angew. Chem. In. Ed.*, 2015, **54**, 7051.
8. (a) E. Muñoz, M. L. R. González, A. S. Ascaso, M. L. Sanjuán, J. M. G. Calbet, M. Laguna and G. F. de la Fuente, *Carbon*, 2010, **48**, 1807; (b) M. B. S. R. Levi, A. A. Yaron, R. P. Biro, C. S. L. Houben, A. Enyashin, G. Seifert, and a. R. T. Yehiam Prior, *J. Am. Chem. Soc.*, 2010, **132**(32): 11214-11222.; (c) J. L. Guo, Y. D. Chiou, W. I. Liang, H. J. Liu, Y. J. Chen, W. C. Kuo, C. Y. Tsai, K. A. Tsai, H. H. Kuo, W. F. Hsieh, J. Y. Juang, Y. J. Hsu, H. J.

Lin, C. T. Chen, X. P. Liao, B. Shi and Y. H. Chu, *Adv Mater.*, 2013, **25**, 2040-2044; (d) L. An, P. Zhou, J. Yin, H. Liu, F. Chen, H. Liu, Y. Du and P. Xi, *Inorg chem*, 2015, **54**, 3281.
9. M. Ye, X. Wen, N. Zhang, W. Guo, X. Liu and C. Lin, *J. Mater. Chem. A*, 2015, **3**(18): 9595-9600.
10. Y. Zhang, X. Li, W. Xu, S. Li, H. Wang and L. S. Li, *Mater. Lett*, 2012, **67**, 117.
11. X. Wang, J. Zhuang, Q. Peng and Y. Li, *Nature*, 2005, **437**, 121.
12. M. S. Zaman, G. B. Grajeda and E. D. Haberer, *J. Appl. Phys*, 2014, **115**, 144311.
13 Y. Rosenfeld Hacohen, R. Popovitz-Biro, Y. Prior, S. Gemming, G. Seifert, and R. Tenne, Phys. Chem. Chem.l Phys. 2003, **5**, 1644.
14 P. Kumar and R. Nagarajan, *Inorg chem*, 2011, **50**, 9204.